Biogeosciences

Supplement of

Forest–atmosphere exchange of reactive nitrogen in a remote region – Part I: Measuring temporal dynamics

**Pascal Wintjen et al.**

Correspondence to: Pascal Wintjen (pascal.wintjen@thuenen.de)

Description of wet deposition measurements

Wet-only and bulk deposition were collected by four samplers, one wet-only and three bulk samplers, at an open site. The measurements took place in southwest direction of the tower (approx. 1.3 km). Bulk samplers had a funnel opening of 321 cm^2 at 1.25 m above ground. The automatic wet-only sampler (NSA 181K – cooled, Eigenbrodt, Königsmoor, Germany) had a funnel opening of 500 cm^2 at 2 m above ground. During the weekly sampling intervals, precipitation samples were kept dark and cool (<4°C). After sampling they were filtered (< 0.45 µm, Whatman) and cooled at 2 to 4°C without chemical preservation/treatment until analysis. No biocides were used during sampling because denitrification was unlikely due to the short exposure time and permanent cooling. In fact, we found very low carbon concentrations and no nitrite as an intermediate product of denitrification in the precipitation samples. NH_4^+ and NO_3^- were analyzed following DIN EN ISO 10304-1. Determination of total wet N was done according to DIN 38409-27 and EN 12260. Dissolved organic nitrogen is calculated by subtracting NH_4^+-N and NO_3^--N from total wet N.
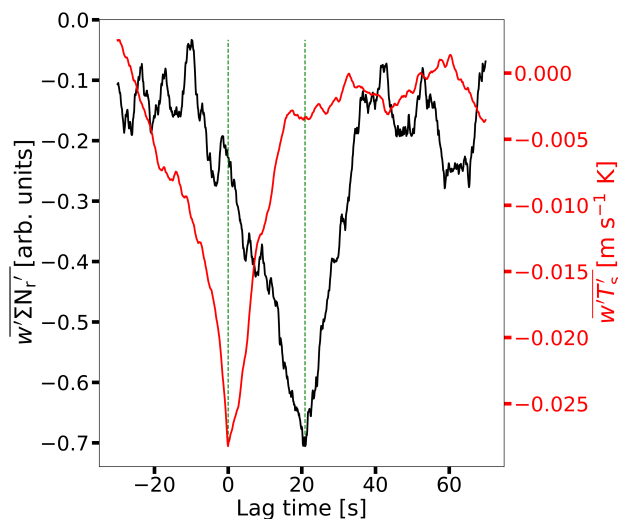

Figure S1. Covariance function of vertical wind and temperature (red) and covariance function of vertical wind and ΣN_r concentration (black). Green, dashed lines indicate the maximum covariance, which is around 20 s for the TRANC-CLD. Data were recorded at the 22 April 2017 from 05:00 to 05:30 LT
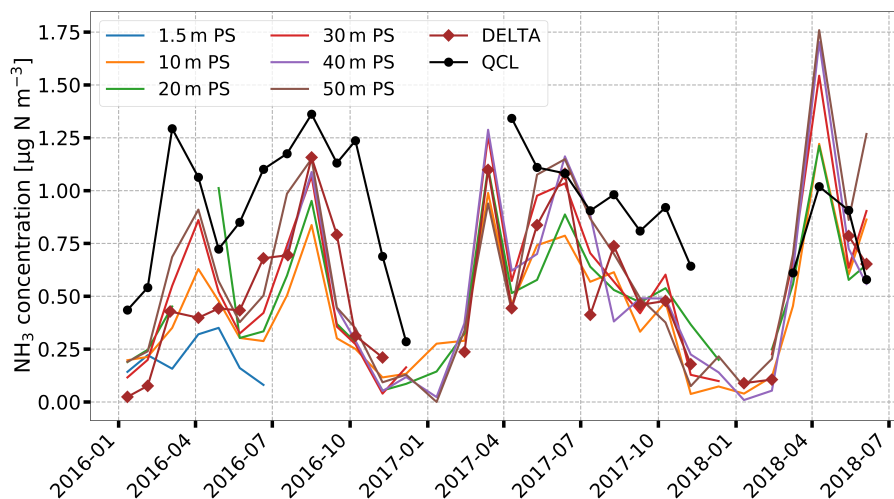
Figure S2. Concentrations of NH$_3$ measured by the DELTA and passive samplers, and the QCL in µg N m^{-3}. NH$_3$ of the QCL was averaged to the exposition period of the long-term samplers. Colors of the passive samplers indicate different measurement heights.
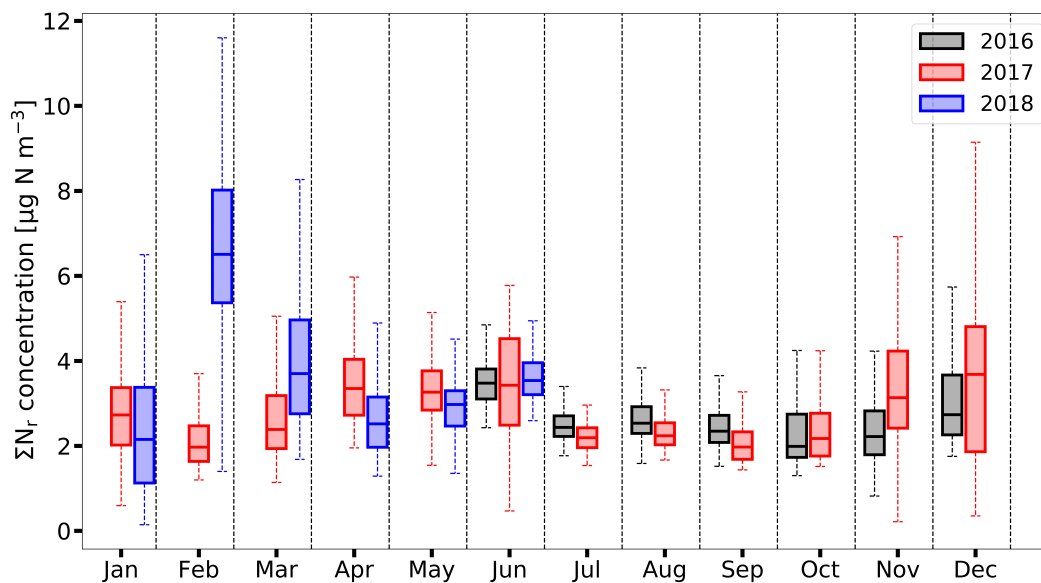

Figure S3. Time series of measured ΣN_r concentrations shown as box-and-whisker plots on monthly basis (box frame = 25% to 75% interquartile ranges (IQR), bold line = median, whisker = 1.5· IQR) in µg N m^{-3}. Colors indicate different years
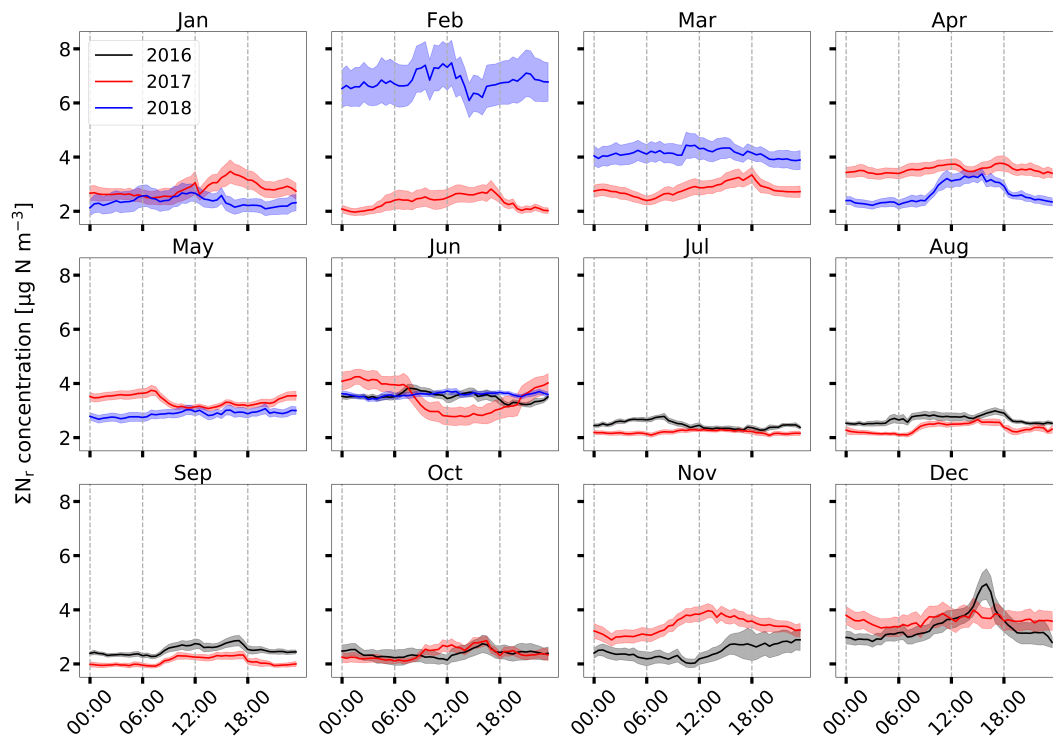
Figure S4. Mean diurnal cycle of ΣN_r concentrations (μg N m^{-3}) based on half-hourly measurements for every month from June 2016 to June 2018. The shaded area represents the standard error of the mean. Colors indicate different years.
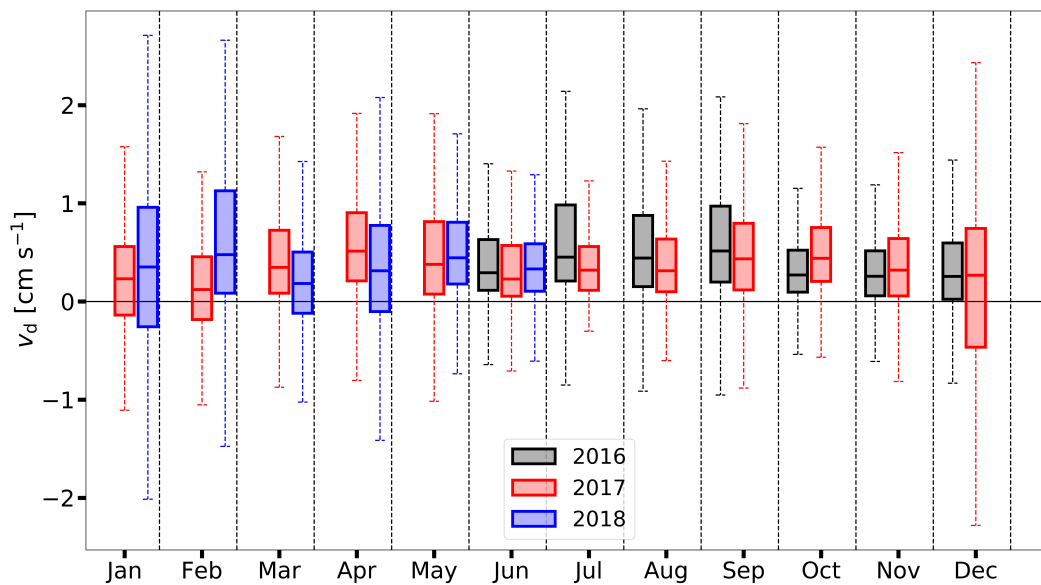

Figure S5. Time series of measured $v_d(\Sigma N_r)$ presented by box-and-whisker plots on monthly basis (box frame = 25% to 75% interquartile ranges (IQR), bold line = median, whisker = 1.5· IQR) in cm s^{-1}. Colors indicate different years.
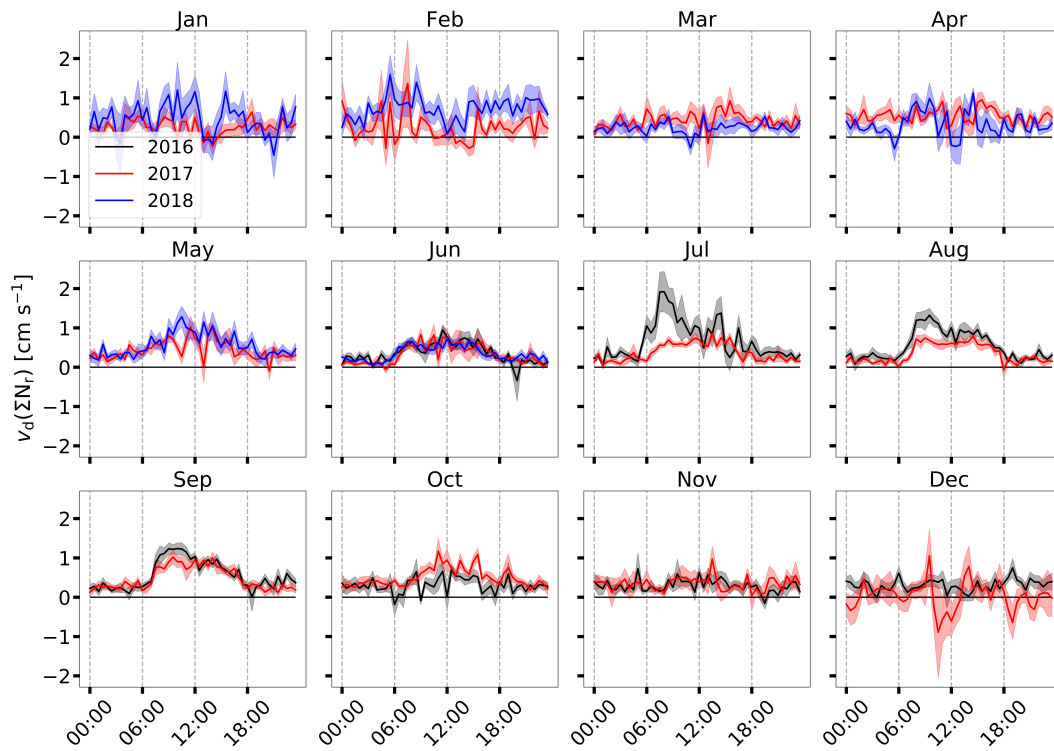
Figure S6. Mean diurnal cycle of $v_d(\Sigma N_r)$ (cm s^{-1}) based on half-hourly measurements for every month from June 2016 to June 2018. The shaded area represents the standard error of the mean. Colors indicate different years.
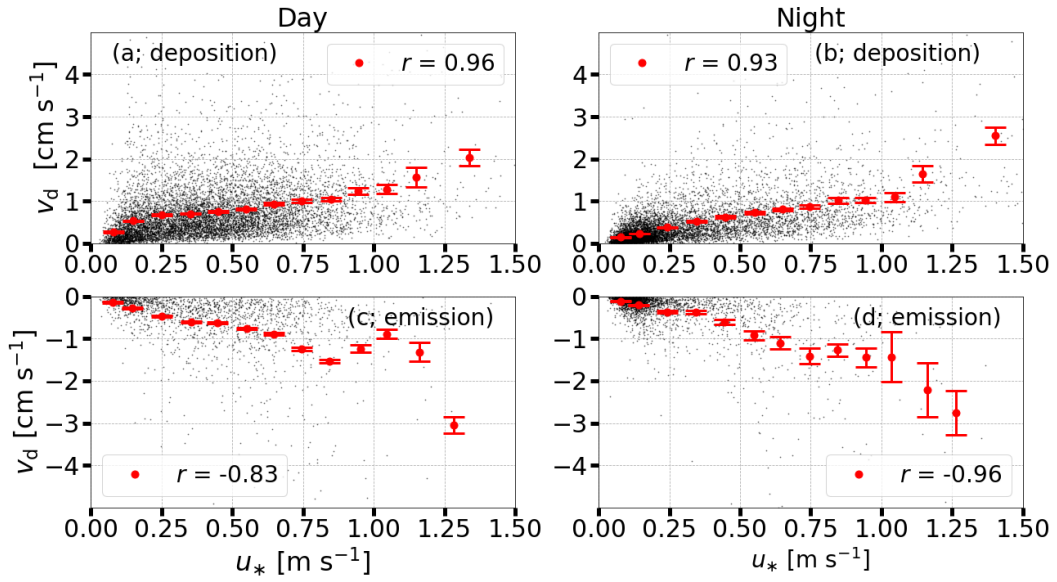
Figure S7. Relationships between measured u_* and corresponding ΣN_r v_d separated in emission and deposition during day ((a) and (c)) and night ((b) and (d)). Half-hourly data is displayed in black, red dots represents averages binned in increments of $0.1\,\mathrm{m\,s^{-1}}$. Error bars indicate the standard error of the averages. The threshold for identifying day and nighttime v_d was set to $10\,\mathrm{W\,m^{-2}}$. r represents the measure of correlation evaluated for the binned data.
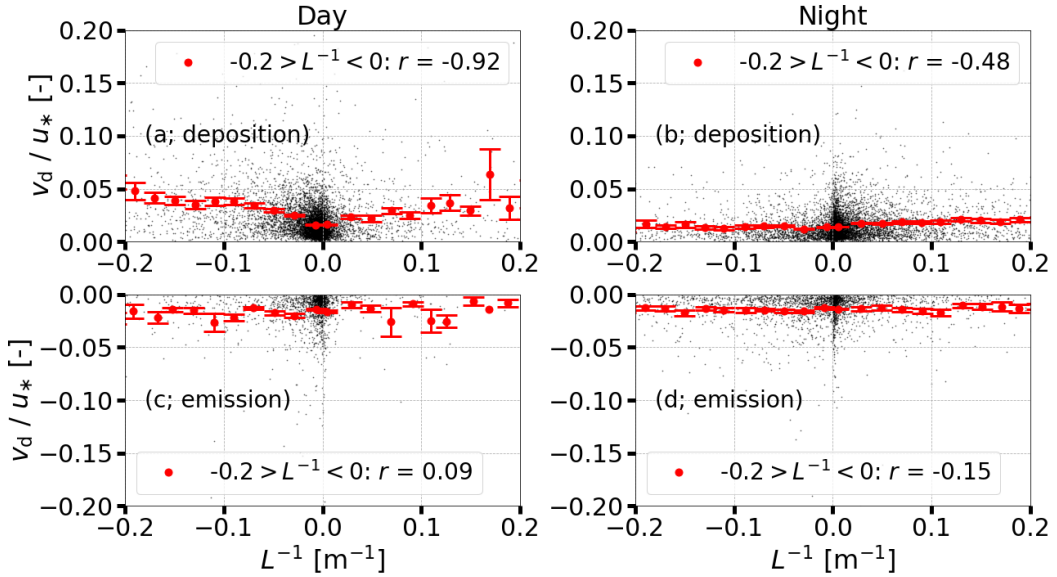

Figure S8. Relationships between L^{-1} and corresponding corresponding ratios v_d/u_* separated in emission and deposition during day ((a) and (c)) and night ((b) and (d)). Half-hourly data is displayed in black, red dots represents averages binned in increments of $0.02\,\mathrm{m^{-1}}$. Error bars indicate the standard error of the averages. The threshold for identifying day and nighttime v_d was set to $10\,\mathrm{W\,m^{-2}}$. r represents the measure of correlation evaluated for the binned data.
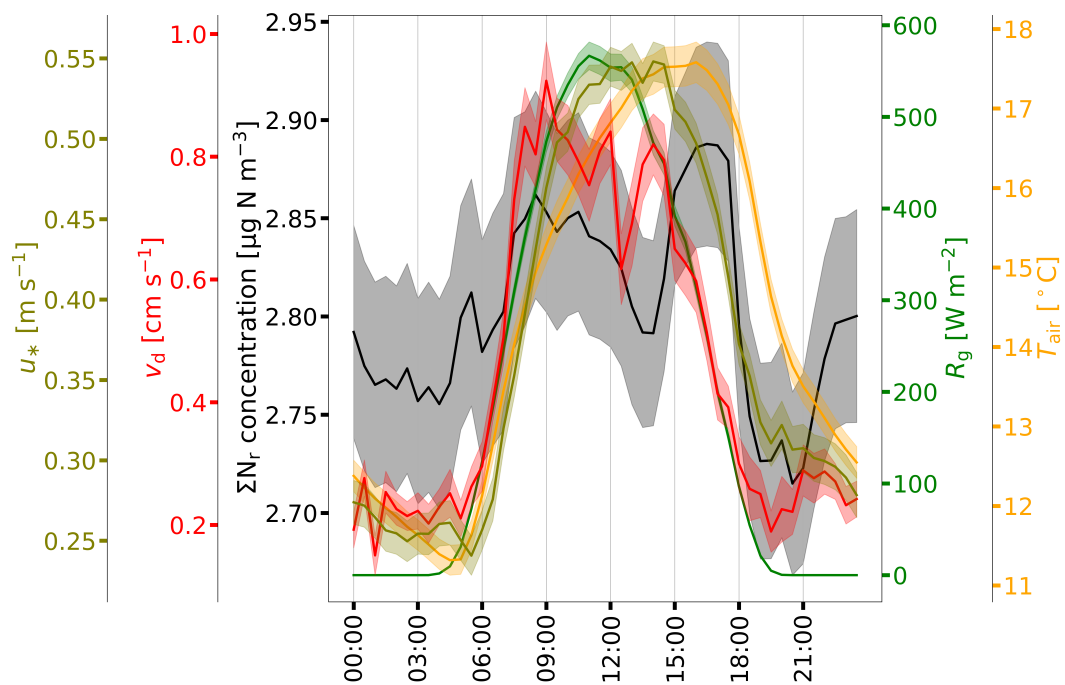
Figure S9. Diurnal cycles of ΣN_r (black) concentration, R_g (green), u_* (olive), air temperature T_{air} (orange), and v_d (red) for the period from May to September. Shaded areas represent the standard error of the mean.
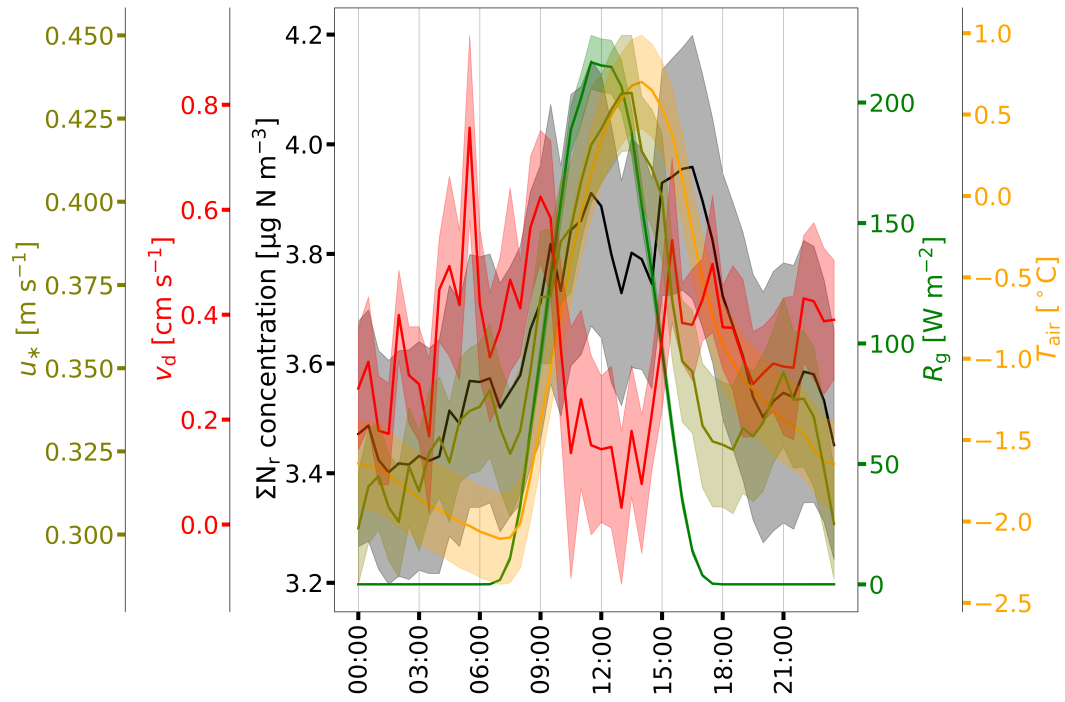
**Figure S10.** Diurnal cycles of ΣN_r (black) concentration, R_g (green), u_* (olive), air temperature T_{air} (orange), and v_d (red) for the period from December to February. Shaded areas represent the standard error of the mean.
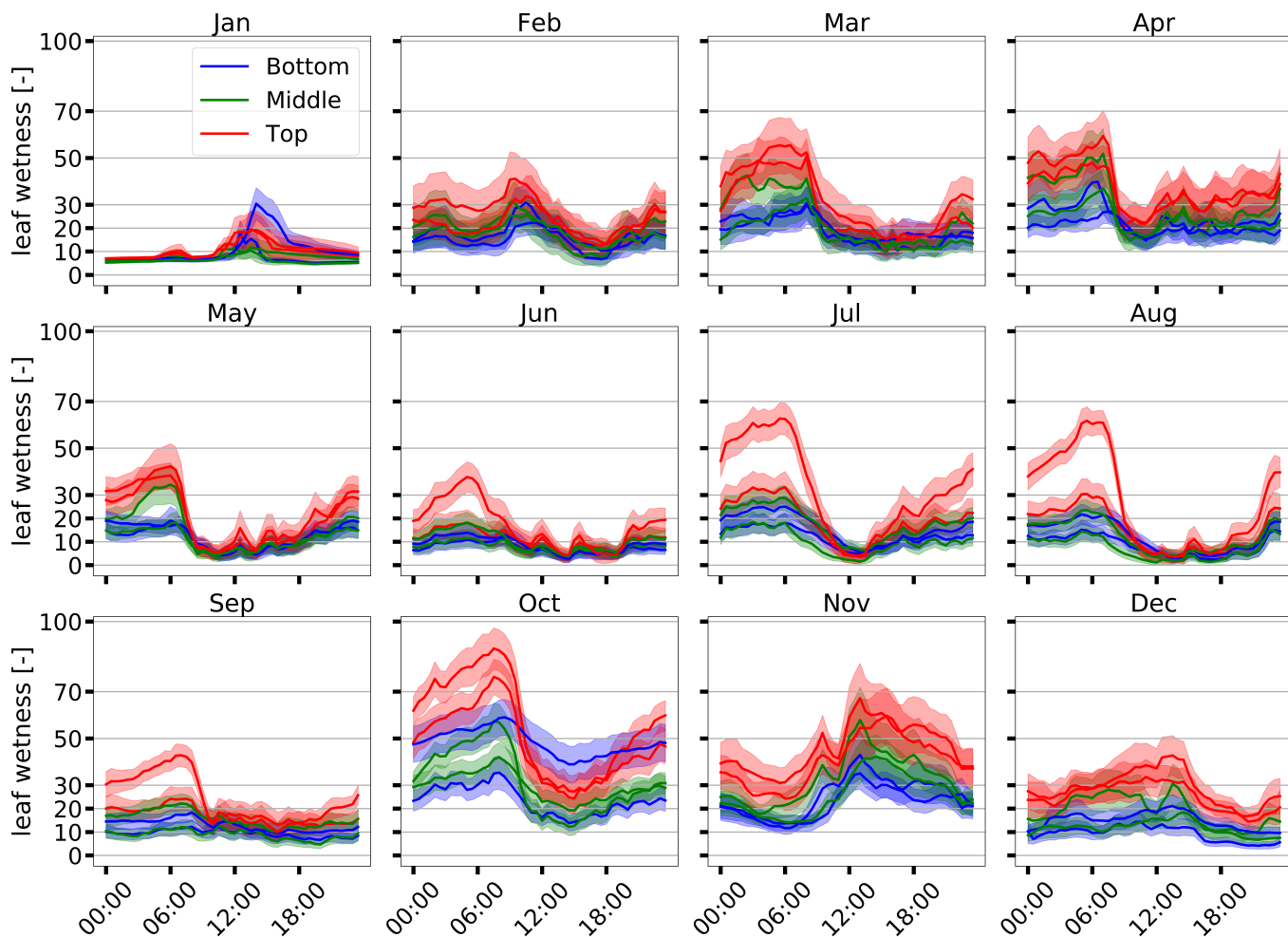
Figure S11. Diurnal cycles of the leaf wetness for 2017. Colors indicate installation heights of the sensors (red=top, green=middle, blue=bottom). Shaded areas represent the standard error of the mean.

Figure S9 shows diurnal cycles of the leaf wetness for all sensors on monthly basis for 2017. On monthly basis, the diurnal patterns of the sensors were almost the same for a season. From April, the start of the growing season, to September highest values were measured during dawn and lowest values during the day. During daylight, only slight differences in measurement height were visible. Considering the standard error, the differences in measurement heights diminished, especially between the lowest and middle sensor. Also, sensors from the mid and the top were within their uncertainty ranges. In conclusion, sensors at the lowest height seem to remain "wet" later during the morning, but effect is within the standard error range. Using only the top sensors for deriving the leaf wetness value, seems not to be appropriate with regard to the uncertainty ranges. Thus, we used all sensors for deriving a wetness boolean, which also lowered its uncertainty.
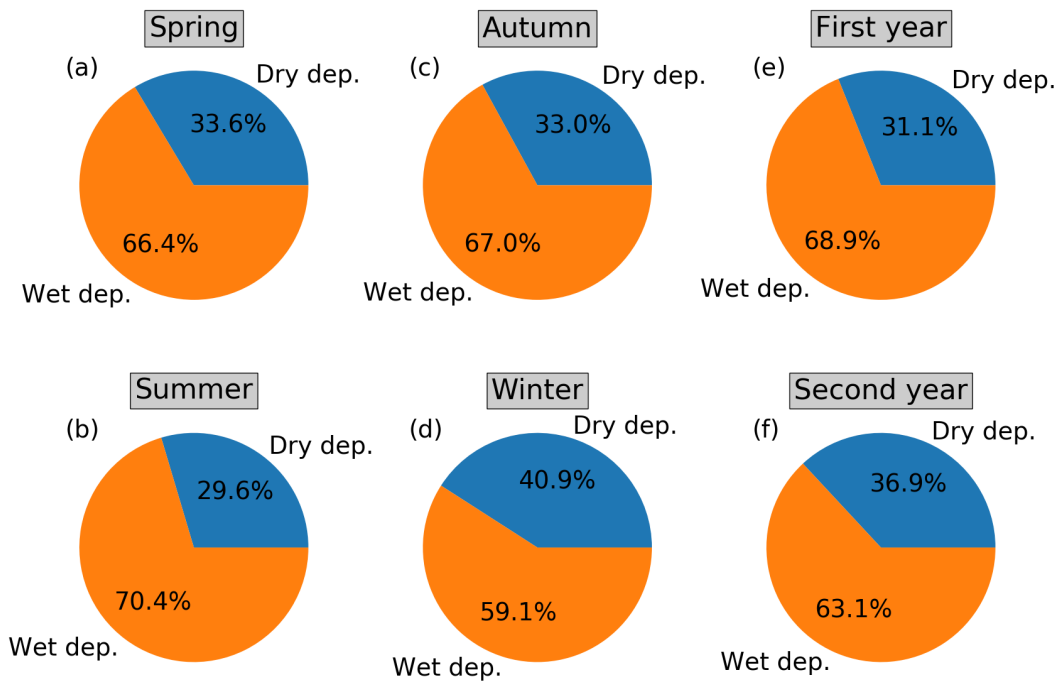
Figure S12. Contribution of dry and wet deposition to total deposition for each season and both measurement years labeled from (a) to (f).
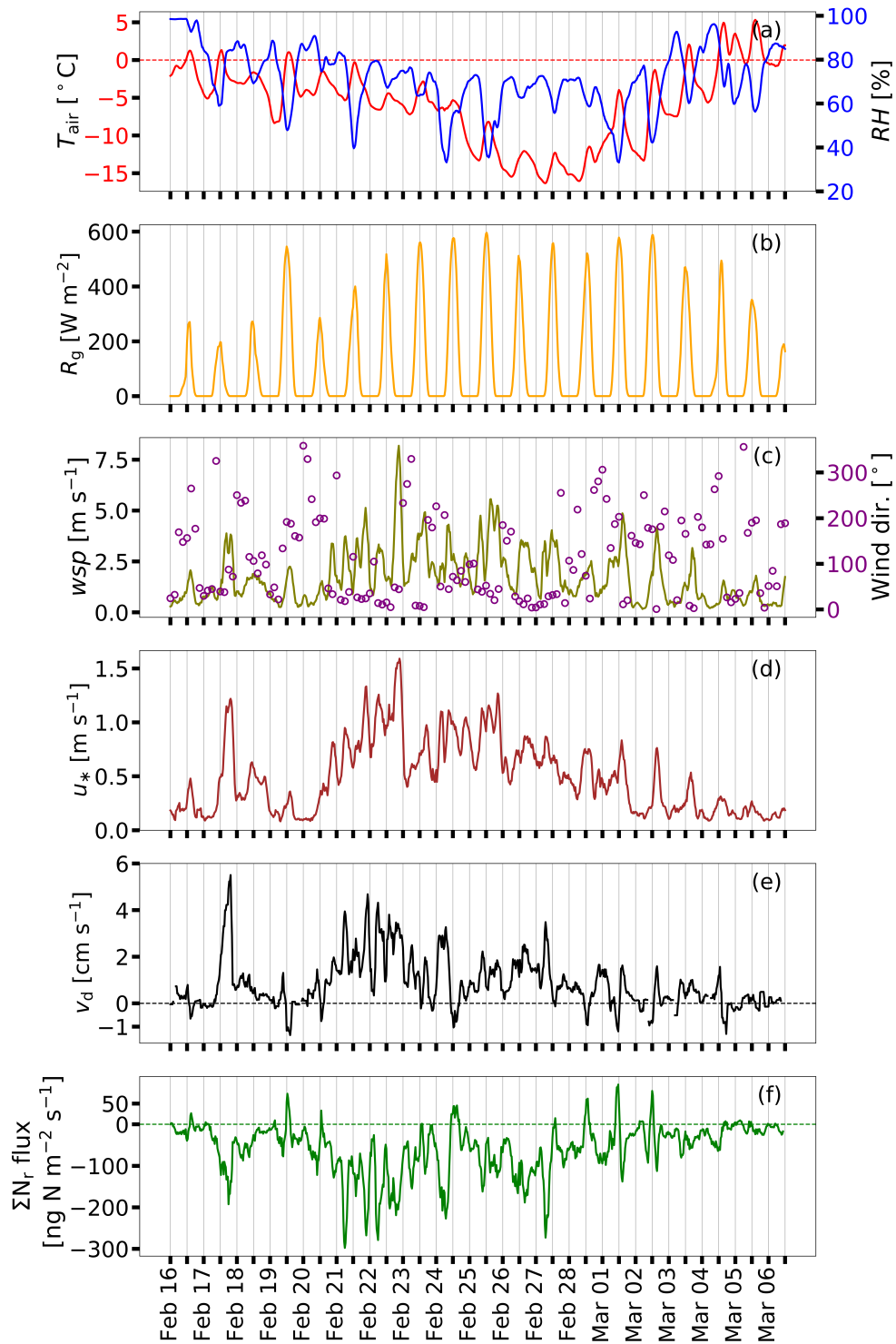
Figure S13. Recorded air temperature (T_{air}), relative humidity (RH), global radiation (R_g), wind speed (wsp), friction velocity (u_*), v_d, and ΣN_r flux as 3-h running mean from 16 February to 6 March 2018. Wind direction corresponds to values measured in three-hourly intervals.